Hybrid Materials from Intermolecular Associations between Cationic Lipid and Polymers

Edla M. A. Pereira, Priscila M. Kosaka, Heloísa Rosa, Débora B. Vieira, Yoshio Kawano, Denise F. S. Petri, and Ana M. Carmona-Ribeiro*

Instituto de Química, Universidade de São Paulo, CP 26077, 05513-970 São Paulo SP, Brazil

Received: February 13, 2008; Revised Manuscript Received: June 2, 2008

Intermolecular associations between a cationic lipid and two model polymers were evaluated from preparation and characterization of hybrid thin films cast on silicon wafers. The novel materials were prepared by spin-coating of a chloroformic solution of lipid and polymer on silicon wafer. Polymers tested for miscibility with the cationic lipid dioctadecyldimethylammonium bromide (DODAB) were polystyrene (PS) and poly(methyl methacrylate) (PMMA). The films thus obtained were characterized by ellipsometry, wettability, optical and atomic force microscopy, Fourier transform infrared spectroscopy (FTIR), differential scanning calorimetry (DSC), and activity against *Escherichia coli*. Whereas intermolecular ion−dipole interactions were available for the PMMA-DODAB interacting pair producing smooth PMMA-DODAB films, the absence of such interactions for PS-DODAB films caused lipid segregation, poor film stability (detachment from the silicon wafer) and large rugosity. In addition, the well-established but still remarkable antimicrobial DODAB properties were transferred to the novel hybrid PMMA/DODAB coating, which is demonstrated to be highly effective against *E. coli*.

Introduction

Supported bilayers have been recognized as models for biological membranes where the structure and function of membrane peptides, proteins, and receptors can be conveniently isolated and reconstituted.[1–9] Several surfaces have been used as supports to deposit the bilayer or adhered bilayer vesicles, for example, glass coverslips for spectroscopic studies,[10] mica sheets for the surface force apparatus,[11–13] polymer-coated surfaces with one or more polymer layers,[14–18] bacteria,[19] yeasts[20] or mammalian cell surfaces,[21] mineral particles such as silica,[22–26] glass beads[27] or titanium dioxide,[28] and polymeric latex particles.[29–31] However, in certain cases, the instability inherent in noncovalently associated lipid films has substantially prevented application of this design. Alternative approaches have been developed such as tethering systems[32] or production of lipid/polymer hybrid films.[33–37]

On the other hand, the deposition of organic monolayers onto solid surfaces containing quaternary ammonium groups has been shown to prevent deposition and growth of bacterial biofilms.[38] Molecules with a net positive charge are able to kill microorganisms both in solution and upon attachment or adsorption to surfaces.[38,39] In particular, the synthetic cationic lipid dioctadecyldimethylammonium bromide (DODAB) exhibits outstanding antimicrobial properties,[19–21,39–41] possibly useful to produce antimicrobial coatings. In this work, spin-coated DODAB, polymeric or polymer-DODAB films on silicon wafers are characterized by means of ellipsometry, contact angle determinations, and atomic force microscopy. Poly(methyl methacrylate) (PMMA) and polystyrene (PS) were chosen as polymers because of their large application field.[42] PMMA has been extensively used in semiconductor research and industry for developing optical and orthopedical devices. PS is economical and has been used for packing, plastic cutlery, CD "jewel" cases, and many others objects where a fairly rigid, economical plastic of any of various colors is desired. Spin-coating has often been used to prepare either lipid [43–50] or polymer films.[51–54] In this work, intermolecular associations between a cationic lipid and two model polymers were evaluated from preparation and characterization of hybrid thin films cast on silicon wafers by spin-coating. Intermolecular carbonyl-quaternary nitrogen interactions for the PMMA-DODAB pair displaced infrared carbonyl absorption by about 4 cm^{-1} and produced smooth PMMA-DODAB films where phase separation was absent as shown from differential scanning calorimetry (DSC) and phase images from atomic force microscopy (AFM). The absence of such interactions for PS-DODAB films caused lipid segregation, poor film stability (detachment from the silicon wafer), and large rugosity. In addition, the well-established but still remarkable antimicrobial DODAB properties were transferred to the novel hybrid PMMA/DODAB coating, which is demonstrated to be highly effective against *E. coli*. The low cost and simple one-step preparation procedure for obtaining the hybrid films would certainly be an invaluable advantage in comparison to many-steps methods such as layer-by-layer or covalent modification of polymeric matrixes. Many applications can be foreseen from DODAB impregnation in polymer matrixes.

Material and Methods

Materials. Polystyrene (PS), 99.5% purity, was supplied by BASF, Ludwigswafen, Germany, and poly(methyl methacrylate) (PMMA), by Sigma-Aldrich, Milwaukee, WI. Dioctadecyldimetilammonium bromide (DODAB) 99.9% purity was purchased from Sigma. Silicon ⟨100⟩ wafers were purchased from Silicon Quest (U.S.A.) with a native oxide layer approximately 2 nm thick that were used as substrates. The wafers are composed of Si and a native layer of SiO_2. They are cut into small pieces with area of approximately 1 cm^2, cleaned with acetone, and finally dried under a stream of N_2 to further use. All other reagents were analytical grade and used without further purification.

* To whom correspondence should be addressed. Phone: 55 11 3091 3810ext 237. Fax: 55 11 3815 5579. E-mail: mcribeir@iq.usp.br.

10.1021/jp801297t CCC: $40.75
Published on Web 07/16/2008

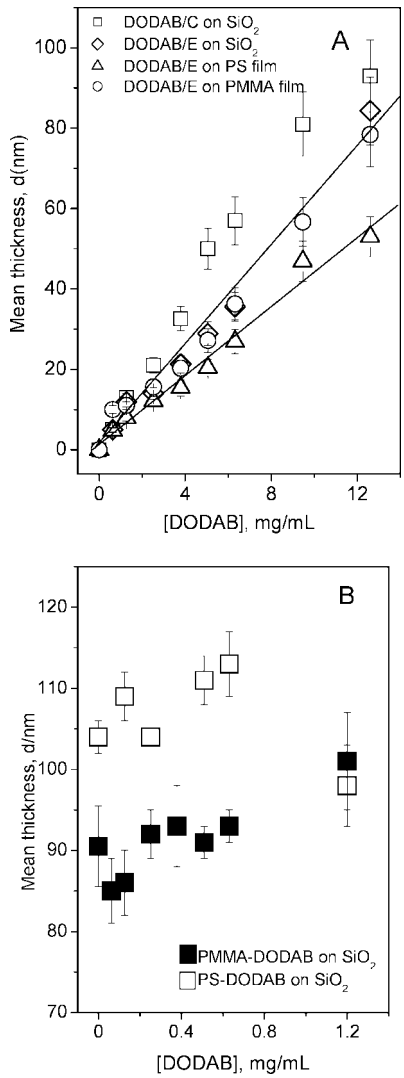

Figure 1. (A) Mean thickness of DODAB films as a function of DODAB concentration. Films were spin-coated from ethanolic (E) or chloroformic DODAB solutions (C). Ellipsometry was employed to determine film thickness d (nanometers). Substrates for film deposition were either SiO_2 or previously spin-coated polymeric coatings of PS or PMMA. The lines represent the linear fits (see eq 24). (B) Mean thickness of polymer-DODAB films as a function of DODAB concentration for films spin-coated on silicon wafers from chloroformic solutions. Error bars represent the mean standard deviation.

Films Preparation. Two experimental approaches have been followed. In the first one, DODAB solutions in ethanol, a good solvent for DODAB, in the concentration range of 0.6 to 12.6 mg/mL were spin-coated onto bare Si wafers or onto polymeric (PMMA or PS) films. Films of PMMA or PS were previously produced by spin-coating onto Si wafers from toluene solutions at 10.0 mg/mL.[52,53] In the second set of experiments, solutions containing DODAB and PS or PMMA were prepared in chloroform, a good solvent for both polymers and DODAB. The solutions were prepared at fixed final concentration of polymer (10 mg/mL) and DODAB concentration varying from 0.1 mg/mL to 6.0 mg/mL. All coatings were obtained by means of a Headway PWM32-PS-R790 spinner (Garland, U.S.A.), operating at 3000 rpm during 40 s, (24 ± 1) °C and (50 ± 5)% of relative humidity.

Ellipsometry. Ellipsometric measurements were performed in the air at (24 ± 1) °C using a vertical computer-controlled DRE-EL02 ellipsometer (Ratzeburg, Germany). The angle of incidence was set at 70.0° and the wavelength, λ, of the He−Ne laser was 632.8 nm. For the data interpretation, a multilayer model composed by the substrate, the unknown layer, and the surrounding medium should be used. Then the thickness (d) and refractive index (n) of the unknown layer can be calculated from the ellipsometric angles, Δ and Ψ, using the fundamental ellipsometric equation and iterative calculations with Jones matrices:[55]

$$e^{i\Delta} \tan \psi = R_p/R_s = f(n,d,\lambda,\varphi) \quad (1)$$

where R_p and R_s are the overall reflection coefficients for the parallel and perpendicular waves. They are a function of the angle of incidence ϕ, the wavelength λ of the radiation, the refractive index (n), and the thickness of each layer of the model (d).

From the ellipsometric angles Δ and Ψ and a multilayer model composed by silicon, a silicon dioxide and spin-coated layer is possible to determine the thickness of the uppermost layer. First of all, the thickness of the SiO_2 layers was determined in air, considering the refractive index for Si as $\tilde{n} = 3.88 - i0.018$[56] and its thickness as an infinite one, for the surrounding medium (air) the refractive index was considered as 1.00. Because the native SiO_2 layer is very thin, its refractive index was set as 1.462[56] and just the thickness was calculated. The mean thickness of the native SiO_2 layer amounted to (1.9 ± 0.2) nm. When the independent determination of n and d was not possible for spin-coated layers (low optical contrast), n was kept as 1.500 for DODAB[53] 1.495 for PMMA,[54] and/or 1.590 for PS,[54] and d was calculated. In the case of hybrid films, the values of n were determined by iterative calculations.

Contact Angle. Measurements were performed at (24 ± 1) °C in a home-built apparatus as previously described.[52,53,56,57] Sessile water drops of 8 μL were used to determine the advancing (Θ_A) contact angle. In order to avoid effects due to adsorbate desorption, measurements of Θ_A took just 5 min.

Atomic Force Microscopy (AFM) and Optical Microscopy. AFM topographic images were obtained using a PicoSPM-LE molecular imaging system with cantilevers operating in the intermittent-contact mode (AAC mode), slightly below their resonance frequency of approximately 290 kHz in the air. All topographic images represent unfiltered original data and refer to scan areas of (5 × 5) μm^2 and (1 × 1) μm^2 with a resolution of (512 × 512) pixels. At least two samples of the same material were analyzed at different areas of the surface. Image processing and the determination of the root-mean-square (rms) roughness were performed by using the PicoScan 5.3.2. software. Optical microscopy was performed by means of a NAVITAR zoom lens system and Ultra TV software.

FTIR and DSC Experiments. Fourier transform infrared spectra (FTIR) were obtained in a Bomen MB100 equipment for solid DODAB powder, PMMA/DODAB films and PMMA films (not shown). Special attention was given to infrared absorption band by the carbonyl moiety at 1741 cm^{-1} in pure PMMA. This absorption band changed to 1737 cm^{-1} or 1738 cm^{-1} for PMMA/DODAB films cast from a 10 mg/mL PMMA and 0.6 mg/mL DODAB solution or from a 10 mg/mL PMMA and 6 mg/mL DODAB solution, respectively (not shown). DSC experiments were carried out in a TA Instruments Q-10 DSC coupled to a TA refrigerating cooling system (RSC) interfaced to the Thermal Analyst 2000 software. Analyses were performed in Al semihermetic cuvettes from −40 up to 200 °C with 10 °C·min^{-1} heating rate, under nitrogen atmosphere.

Organism, Culture Conditions and Bacteria Viability Assay. ***Escherichia coli.*** ATCC 25922 was reactivated for 2−5 h at 37 °C in 3 mL of tryptic soy broth, TSB (Merck KGaA, Darmstadt, Germany). Thereafter, bacteria were spread on plates

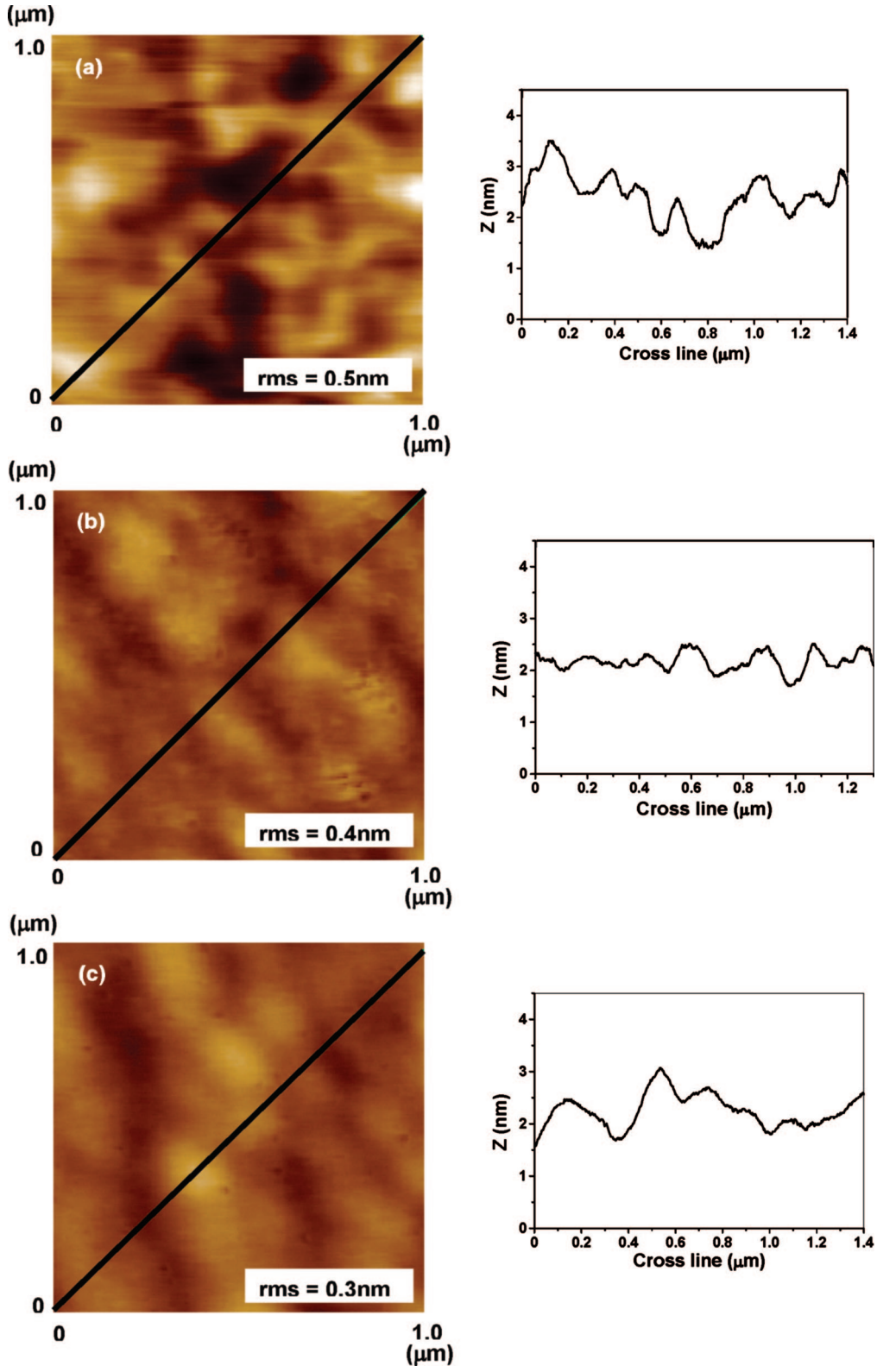

Figure 2. AFM topographic images of DODAB films spin-coated from ethanolic solution at 0.6 mg/mL onto (a) Si wafers, (b) PS (~110 nm thick) and (c) PMMA (~90 nm thick), $Z = 4.5$ nm.

of MacConkey agar (Merck KGaA, Darmstadt, Germany) and incubated (37 °C/6 h). Several colonies were then taken from the plates and incubated in 50 mL of liquid TSB (160 rpm, 37 °C, 2.5 h). The culture was pelleted and separated from its nutritive medium by centrifugation (3000 rpm/5 min). The supernatant was replaced by sterile water and the bacteria pellet was resuspended. The centrifugation/resuspension procedure was repeated three times before using the bacteria for evaluating antimicrobial effects of hybrid polymer/DODAB films. After washing, the final pellet was resuspended in a sterile water volume sufficient to yield 0.9 absorbance unities at 670 nm. The live/dead BacLight™ bacterial viability kit L-7007 (Molecular Probes, Inc., U.S.A.) containing a fluorescent dyes mixture (0.75 μL) was added to 250 μL of the final cell

TABLE 1: Film Characteristics[a]

film	d/nm	n	Θ_A/ °	rms/nm
DODAB (0.6 mg/mL)	7.1 ± 0.1	1.500 ± 0.005	59 ± 3	0.5[(a)]
PMMA	91 ± 1	1.499 ± 0.004	76 ± 5	0.3[(a)]
PMMA-DODAB (0.6 mg/mL)	95 ± 4	1.493 ± 0.004	70 ± 2	0.4[(a)]
PMMA-DODAB (6.0 mg/mL)	114 ± 5	1.501 ± 0.006	50 ± 5	3[(b)]
PS	104 ± 2	1.599 ± 0.007	84 ± 2	0.6[(a)]
PS-DODAB (0.6 mg/mL)	113 ± 4	1.582 ± 0.005	62 ± 3	1.4[(a)]
PS-DODAB (6.0 mg/mL)	55 ± 6	1.537 ± 0.007	50 ± 2	10[(a)]

[a] Mean values of index of refractive (n) and thickness (d) obtained from iterative calculation, advancing contact angle (Θ_A) and mean surface roughness (rms) for (a) (1 × 1) μm^2 and (b) (5 × 5) μm^2 images. Hybrid films were spin-coated from solutions of DODAB (at 0.6 mg/mL or 6.0 mg/mL) and polymer (PMMA or PS at 10 mg/mL) in chloroform. For comparison, the characteristics of pure PMMA or PS films prepared from solutions at 10 mg/mL in chloroform are also presented. Mean roughness values (rms) are the mean values calculated from measurements for five different films with the corresponding standard deviation.

suspension and incubated in the dark for 15 min. An aliquot of 0.004 mL of this last mixture was then spread on control and test films coating glass coverslips. Within 1 h after spreading cells on films, fluorescence microscopy coupled to imaging by a CCD digital camera were employed for photographing fluorescent cells upon excitation at 470 nm. Live bacteria are stained fluorescent green by SYTO 9 stain whereas dead bacteria become fluorescent red by propidium iodide. Controls were bare glass coverslips or spin-coated PMMA films previously immersed in 0.1% w/v polylysine solution for 20 min and washed three times in double-distilled water. This last procedure was important to immobilize the bacterial cells at the control surfaces via electrostatic attachment. DODAB/PMMA films were used as test films without previous coverage with polylysine since the hybrid films were expected to already be cationic and able to immobilize cells by themselves without any need of polylysine.

Results and Discussion

DODAB Films onto Si Wafer or PMMA or PS Films. DODAB solutions in ethanol (E) were spin-coated onto silicon wafers or onto preformed PMMA or PS films. Figure 1A shows the dependence of mean ellipsometric DODAB film thickness (d) on DODAB concentration, which allows prediction of film thickness given a DODAB concentration and a substrate. The data could be fitted with linear regressions:

$$d = (6.7 \pm 0.2)c_{DODAB} \quad R = 0.9915 \text{ for bare Si wafer} \quad (2)$$

$$d = (6.3 \pm 0.1)c_{DODAB} \quad R = 0.9930 \text{ for PMMA films} \quad (3)$$

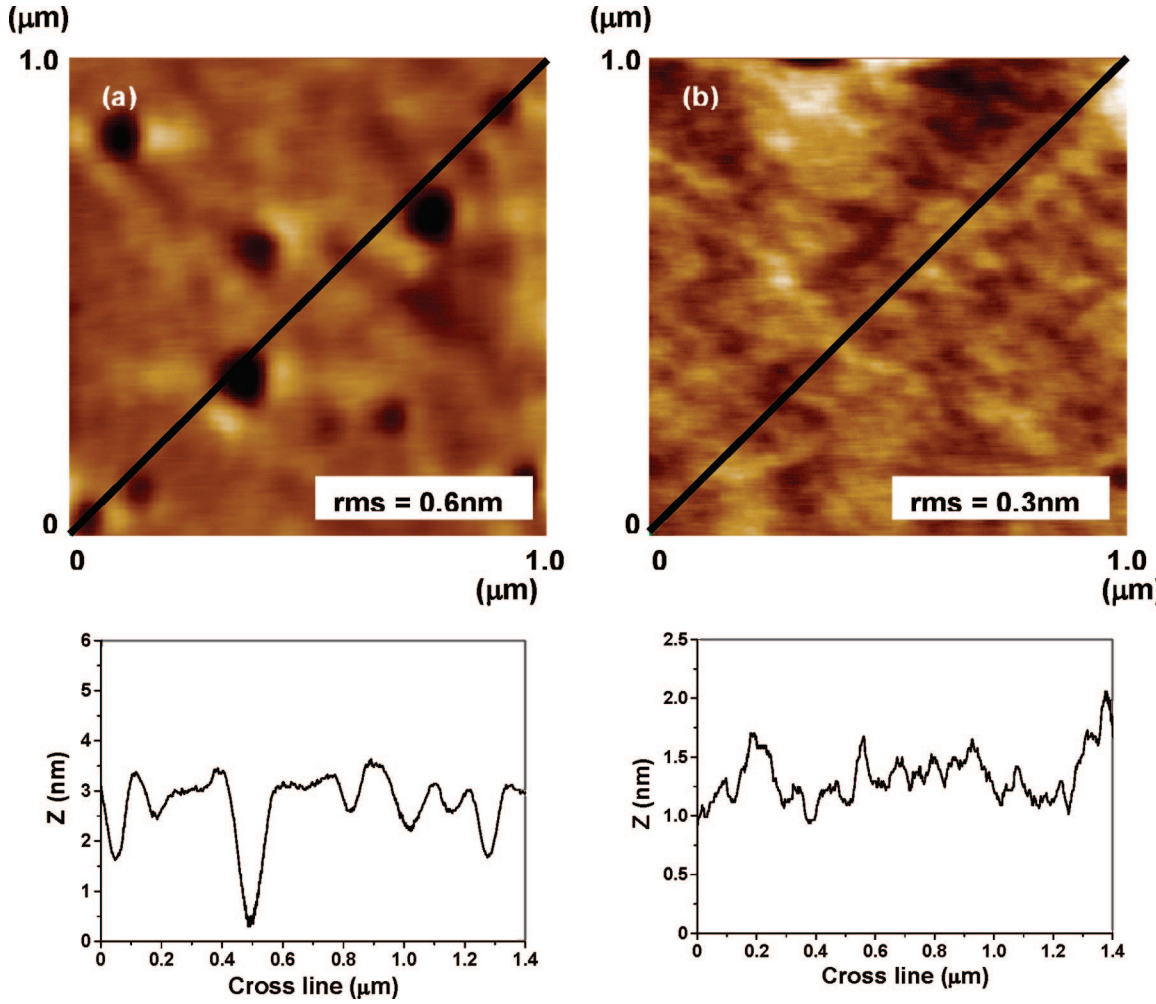

Figure 3. AFM topographic images of polymer films spin-coated form chloroform solution at 10 mg/mL (a) PS, $Z = 6$ nm and (b) PMMA, $Z = 2.5$ nm.

$$d = (4.4 \pm 0.4)c_{DODAB} \quad R = 0.9914 \text{ for PS films} \qquad (4)$$

The angular coefficient d/c_{DODAB} from eq 24 tends to decrease with the substrate hydrophobicity. The highest d/c_{DODAB} value was observed for Si/SiO_2, with advancing contact angle (Θ_A) of 5°, while the lowest d/c_{DODAB} value was found for PS with Θ_A of ~80°. This trend evidence packing and/or orientation of DODAB molecules is driven by the substrate nature. Although PMMA substrates are less hydrophilic surfaces ($\Theta_A \sim 70°$) than Si/SiO_2, d/c_{DODAB} found in eqs 2 and 3 were similar, indicating favorable interaction between PMMA carbonyl groups and DODAB polar heads (strong ion−dipole interaction). Figure 1B shows the dependence of mean layer thickness of hybrid PMMA-DODAB or PS-DODAB films on DODAB concentration.

Figure 2 presents topographic images of DODAB (0.6 mg/mL) onto Si/SiO_2, PS, and PMMA, with the corresponding cross sections. Regardless of the substrate, DODAB films are smooth and present similar surface roughness (rms values).

DODAB film stability was evaluated from percent desorption calculated from the ratio between mean film thickness, measured in air, after immersion in pure water during 24 h and mean film thickness previously determined in air. DODAB films deposited on PMMA or PS films presented (60 ± 10)% desorption in water, while DODAB onto Si wafers desorbed approximately (80 ± 20)%. Thus, DODAB desorption from both surfaces is the same considering the limits of the experimental error. Spin-coated natural lipids onto silicon, glass,[43] or mica[46] substrate also formed smooth layers which detached upon immersing into water.

Hybrid Films of PMMA-DODAB or PS with High DODAB Content (6 mg/mL). Characteristics of hybrid films of DODAB and PMMA or PS spin-coated onto Si wafers are presented in Table 1. For comparison, the characteristics of pure PMMA or PS films are also presented. The mean refractive indexes, n, values determined from iterative calculations and experimental ellipsometric data for hybrid films presented exponential dependence with the composition, which allows prediction of refractive indexes given the composition of the solution components (see Supporting Information) and indicates repulsive interactions between DODAB and PS in the mixtures, since a linear dependence would evidence an ideal mixture.[60] The values of n of PS and DODAB differ within ~0.1. This tendency could not be evidenced for hybrid films of PMMA and DODAB because the indices of refraction of PMMA and DODAB are similar.

Thickness uniformity and morphology of spin-coated films might be affected by solvent evaporation rate[51] or solvent affinity for the substrate.[54] Walsh observed that PMMA films prepared from toluene were more homogeneous than those prepared in chloroform, because toluene has a slower evaporation rate.[51] On the other hand, acid−base interaction between solvent and substrate, as in the case of chloroform and Si/SiO_2, causes competition between polymer and solvent for the substrate, reducing film uniformity.[54] Figure 3 shows PS (rms = 0.6 nm) and PMMA (rms = 0.3 nm) films produced from chloroform solutions. Although chloroform might bring about some defects in spin-coated polymeric films, the hybrid films of PMMA or

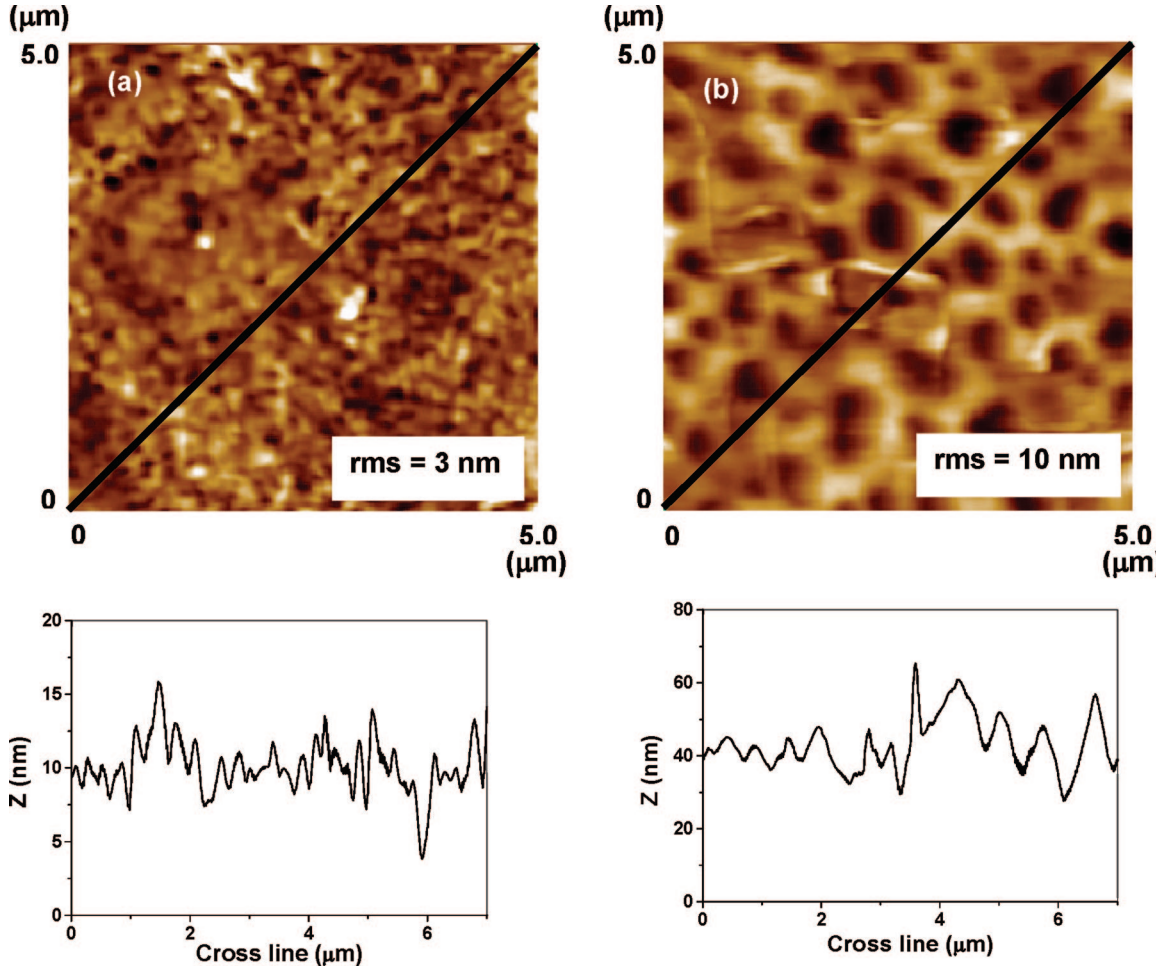

Figure 4. AFM topographic images of hybrid polymer-DODAB films spin-coated from chloroform solution at high DODAB content (6 mg/mL) (a) PMMA-DODAB, Z = 20 nm and (b) PS-DODAB, Z = 80 nm.

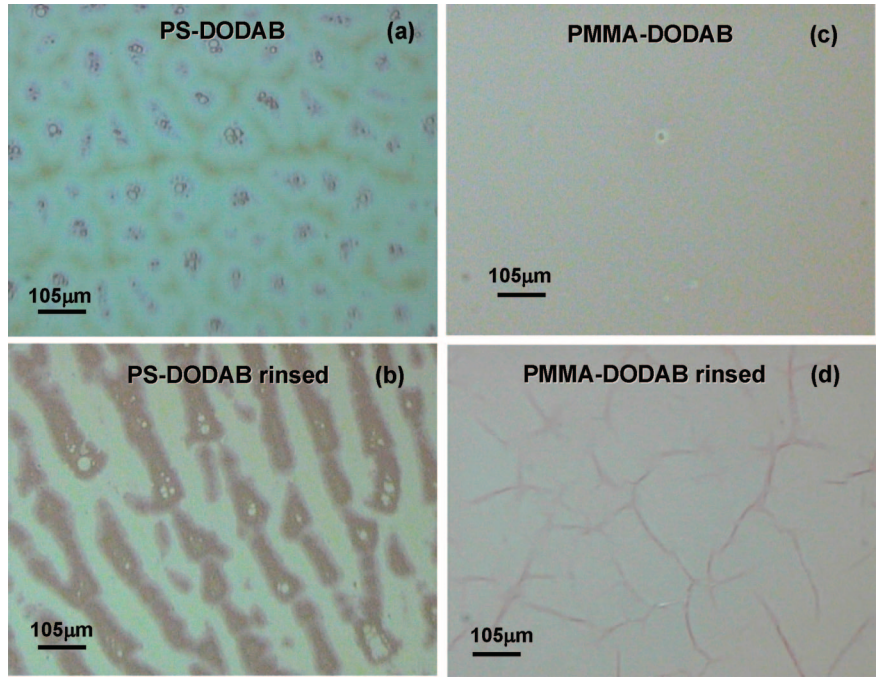

Figure 5. Optical microscopy of hybrid polymer-DODAB films at high DODAB content (6 mg/mL) (a) PS-DODAB, (b) PS-DODAB rinsed with ethanol, (c) PMMA-DODAB, and (d) PMMA-DODAB rinsed with ethanol.

PS and DODAB were prepared from solutions in chloroform, because it is a good solvent for both lipid and polymer and it was available.

Hybrid films of PMMA-DODAB or PS-DODAB with 6 mg/mL of DODAB presented different morphologies. Figure 4a presents a typical AFM topographic image of PMMA-DODAB with the corresponding cross section. PS-DODAB hybrid films presented highly porous structure (Figure 4b; rms = 10 nm), which might be due to phase separation between PS and DODAB and/or to the segregation of DODAB phase at the solid−air interface. In fact, this segregation between PS and DODAB was observed from the nonideal dependence obtained for n on PS content in the mixture and from the AFM phase images (see Supporting Information). PS-DODAB films were also observed by optical microscopy just after the preparation (Figure 5a) and after rinsing under ethanol stream (Figure 5b), a selective solvent for DODAB. Just after the preparation, large domains of phase separation could be observed, where the dark spots were attributed to the DODAB phase because they are the minor component in the mixture (Figure 5a). Figure 5b clearly shows that material has been dragged from the surface after rinsing under ethanol stream, evidencing the presence of DODAB at the solid−air interface. As a control, the same procedure has been done for PMMA-DODAB hybrid films. The morphological features were completely different from those observed for PS-DODAB. Just after the preparation, the surface is homogeneous (Figure 5c); after rinsing under ethanol stream, cracks appeared on the surface (Figure 5d), probably because of dissolution of a miscible phase of DODAB and PMMA, but there was no evidence of DODAB phase separation or DODAB segregation at the solid−air interface, as observed for PS-DODAB. Advancing contact angle (Θ_A) values (Table 1) indicated that the hybrid films are more hydrophilic than pure polymer films, evidencing the presence of DODAB at the solid−air interface. This porous structure facilitates film detachment under water,[59] however, it might be useful for template building (the porous diameter is in average 350 nm). PMMA-DODAB hybrid films are stable under water presenting small roughness values (rms) and the absence of the porous structure observed for PS-DODAB films.

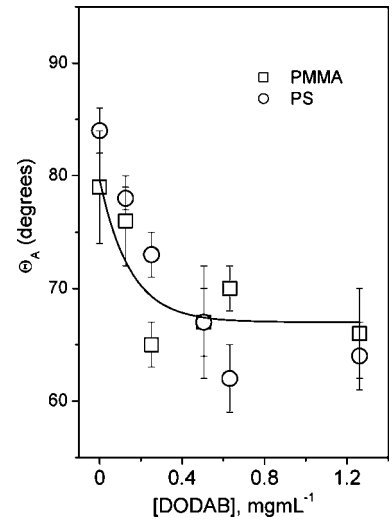

Figure 6. Advancing contact angle (Θ_A) as a function of DODAB concentration for hybrid PMMA-DODAB or PS-DODAB films. Error bars represent the mean standard deviation.

Hybrid Films of PMMA-DODAB or PS-DODAB with Low DODAB Content (0.6 mg/mL). The mean layer thicknesses of spin-coated hybrid DODAB-PMMA films as a function of DODAB concentration (0−1.3 mg/mL or 0−11.5 wt %) in the mixture observed for the hybrid film (PMMA-DODAB) is about (95 ± 4) nm thick, and for the hybrid (PS-DODAB) film, it is around (113 ± 4) nm thick. Both hybrid film surfaces yielded smaller contact angles in comparison to those obtained for the pure PMMA or PS films as shown from the dependence of the advancing contact angle for the films on DODAB concentration (Figure 6). Pure polymer films are more hydrophobic than hybrid polymer-DODAB films (Table 1 and Figure 6).

One should notice that among the organic solvents used to dissolve lipid, polymer, or both, only chloroform dissolves both

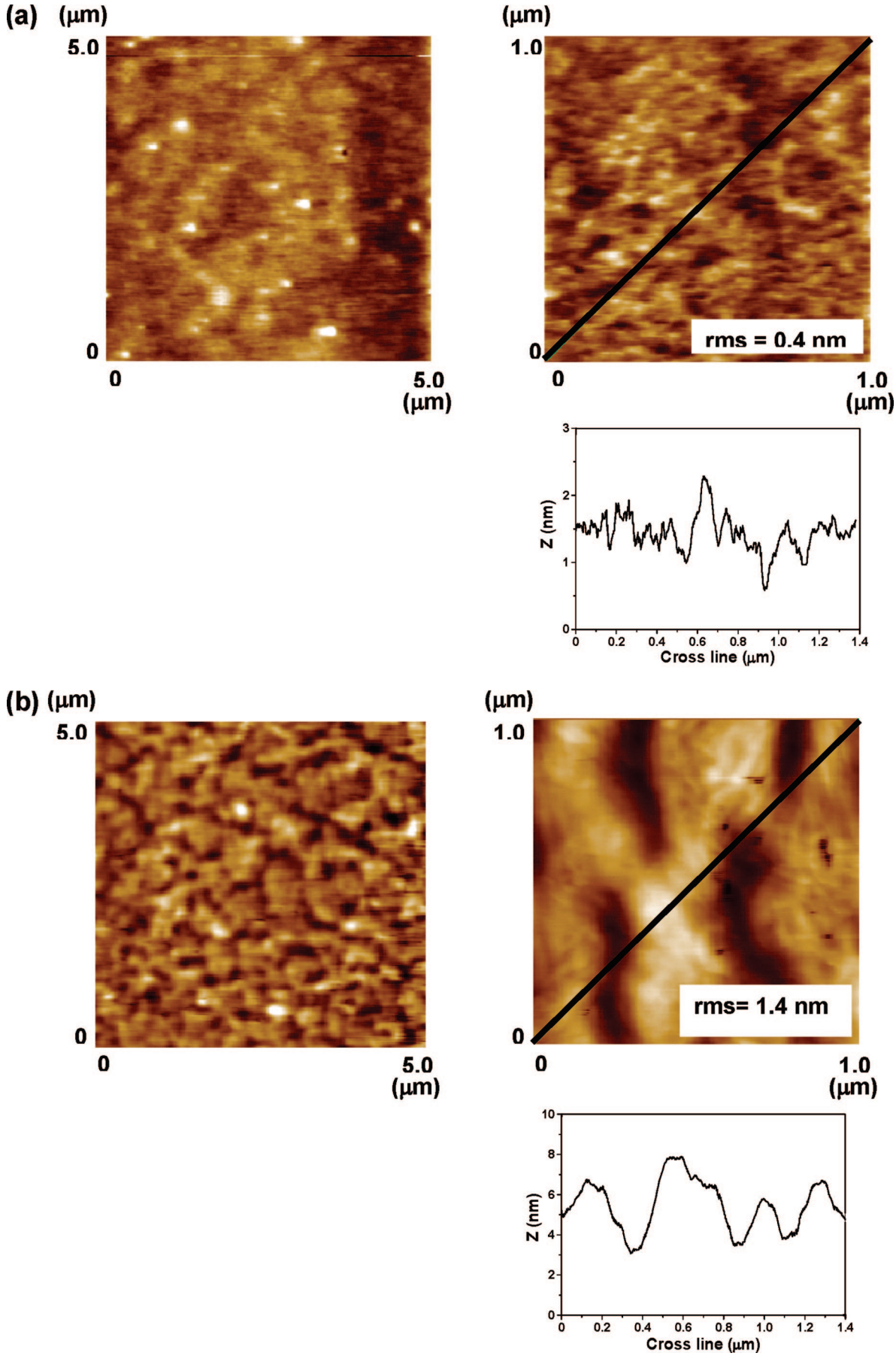

Figure 7. AFM topographic images, (5 × 5) μm^2 and (1 × 1) μm^2, of hybrid polymer-DODAB films spin-coated from chloroform solution at low DODAB content (0.6 mg/mL) (a) PMMA-DODAB, $Z = 3$ nm and (b) PS-DODAB, $Z = 10$ nm.

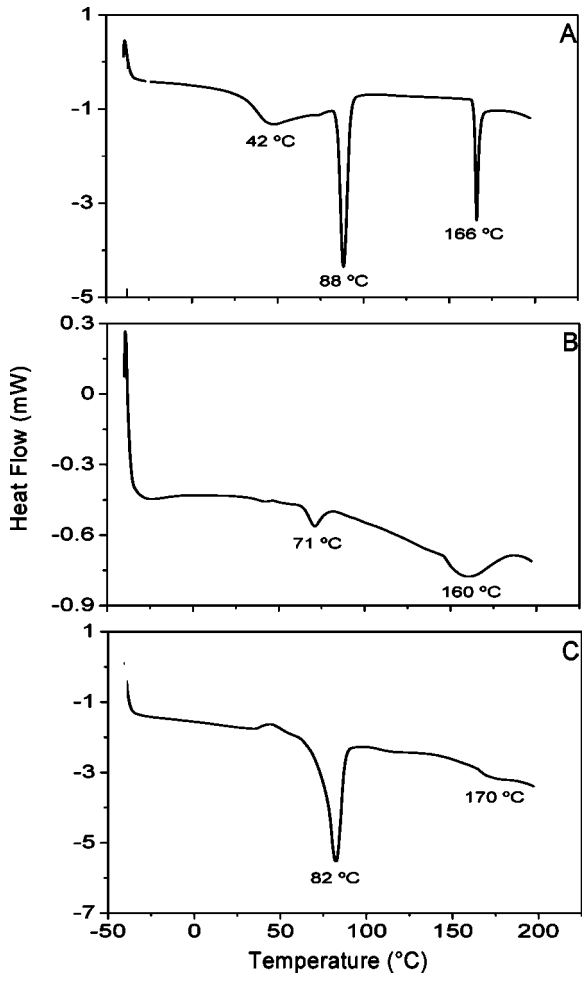

Figure 8. Thermal behavior from DSC curves for pure DODAB powder (A) and PMMA/DODAB film spin-coated from a 10 mg/mL PMMA plus 0.6 mg/mL DODAB (B) or plus 6 mg/mL DODAB chloroformic solution (C).

lipid and polymer so that this was the solvent of choice to prepare the hybrid polymer−lipid films. The rms values for PS-DODAB and PMMA-DODAB films (hybrid films) are 1.4 and 0.4 nm, respectively. PMMA and PS films spread from toluene (T) solutions are smooth presenting low rms values, 0.4 and 0.2 nm,[54] respectively. Depositing lipid films from a lipid ethanolic solution onto preformed PMMA and PS coatings produced relatively smooth films with 0.3 and 0.4 of rms, respectively (Figure 2). However, these coatings had low stability in water in contrast to the hybrid PMMA-DODAB film.

Hybrid films of PMMA-DODAB or PS-DODAB with very low DODAB content (0.6 mg/ml) are very smooth. Figure 7 shows AFM topographic images of hybrid PMMA-DODAB films (Figure 7a) and of PS-DODAB films (Figure 7b). The former is smoother than the latter. Advancing contact angles (Θ_A) for hybrid films, PMMA-DODAB with $\Theta_A = 70 \pm 2$ and PS-DODAB with $\Theta_A = 62 \pm 3$, are smaller than those for pure polymer films, PMMA with $\Theta_A = 79 \pm 5$ and PS with $\Theta_A = 84 \pm 2$, suggesting a change of film−air interfacial properties due to the presence of the lipid in the composite. The exposure of some quaternary ammonium moieties from the lipid at the film−air interface explains the decrease of the contact angle shown in Figure 5.

DSC provided information to support the hybrid nature of PMMA/DODAB films as seen in Figure 8. Pure solid DODAB revealed interesting melting behavior by DSC (Figure 8A). Pronounced endothermic peaks at 88 and 166 °C correspond to van der Waals interaction between DODAB hydrocarbon chains and ionic interactions between DODAB polar heads, respectively (Figure 8A). Curiously, a weaker interaction between hydrocarbon chains in the DODAB solid was detected around 39 °C which can be ascribed to transitions from a more tightly packed to a less tightly packed state of adjacent hydrocarbon chains similar to the gel-to-liquid-crystalline phase transition previously observed for DODAB bilayers in water.[9] DSC for hybrid PMMA/DODAB films shows the disappearance of DODAB typical melting features (Figure 8B,C). Specifically, the ionic interaction between DODAB molecules in the DODAB solid

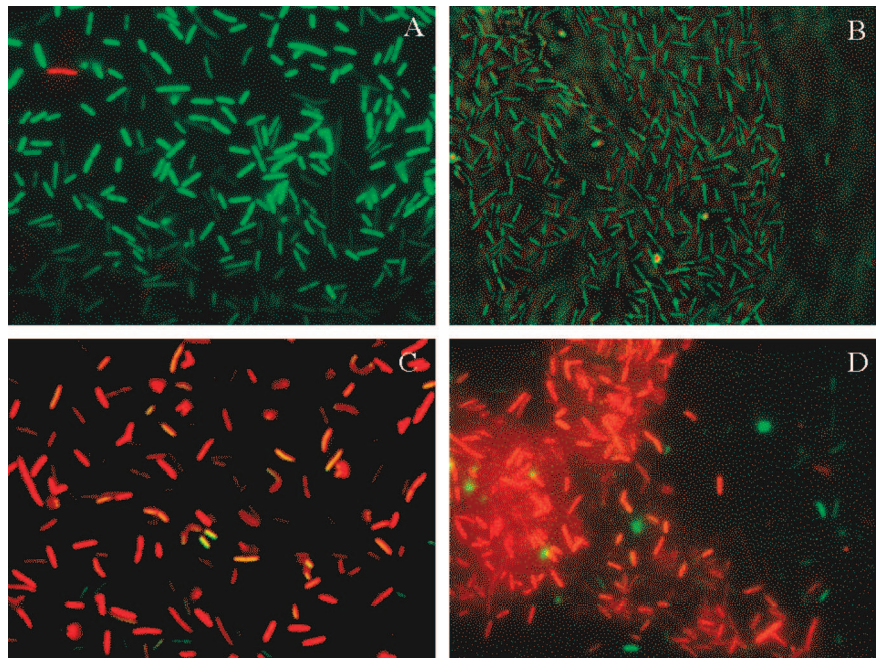

Figure 9. *E. coli* cells on glass coverslips (A); PMMA film (B); hybrid PMMA-DODAB film from 0.6 (C) or 1.2 mg/mL DODAB chloroformic solution (D).

vanished completely in agreement with FTIR data indicating the ion−dipole interaction between quaternary nitrogen in DODAB polar head and carbonyl moiety in PMMA. Indeed, FTIR spectra evidenced a weaker carbonyl stretching in the presence of DODAB (see Materials and Methods). At the higher DODAB/PMMA ratio (Figure 8 C), intermolecular associations between DODAB molecules reappear around 83 °C, suggesting a certain extent of phase separation between DODAB and PMMA. However, ionic clusters in solid DODAB did not reappear even at the quoted high DODAB/PMMA proportion (Figure 8C). The amorphous nature of PMMA yielded the well-known glass transition around 99 °C (not shown) in good agreement with the literature.[56]

Effect of Hybrid DODAB/PMMA Films on *E. coli* Cell Viability. Determination of cell viability of *E. coli* on contact with controls or test PMMA-DODAB films revealed the very effective microbicidal activity of the hybrid film which amounted to total loss of cells viability (Figure 9). Alive cells were observed in green, whereas dead cells were seen in red, according to the BacLight Live Dead L-7007 kit. The controls for cells observed on glass coverslip or on pure PMMA film showed 100% alive cells (all cells in green) at 1 h of interaction time between bacteria and surfaces. The test experiments on PMMA-DODAB hybrid films showed 0% of viable cells (all cells in red) for films spin-coated from 0.6 or 1.2 mg/mL DODAB and 10 mg/mL PMMA. Two mechanisms for the loss of bacterial viability on quaternary ammonium compounds have been suggested. Positively charged surfaces would displace divalent cations such as calcium or magnesium which hold together the negatively charged surface of the lipopolysaccharide network thereby disrupting the outer membrane of *E. coli*[61] or important membrane proteins and channels could have had their conformation and function hampered from direct interactions with the cationic DODAB polar head.[40] Interactions between very potent bactericides such as DODAB liposomes and bacteria did not cause liposome disruption or bacterial cell lysis,[19] but a clear relationship was reported between cell positive charge and loss of cell viability.[62] Positive controls for DODAB bactericidal effect against several pathogenic species are available in the literature for DODAB aqueous dispersions.[40] Combining DODAB directly into a polymer material may provide several advantages as a DODAB delivery mechanism. First, only the necessary amount of DODAB should be used and further systematic studies on dose−response will probably prove high effectiveness of the hybrid material at even lower DODAB doses. Second, DODAB would not leak from the films given its high compatibility with the PMMA matrix. Third, if a polymer material containing DODAB was made from an edible and/or biodegradable polymer, environmental advantages associated with disposal, landfill waste, breakdown, etc, would be realized.[63] The one-step coating for obtaining the hybrid films would be simple and inexpensive in comparison to available technologies. Many applications can be foreseen from DODAB impregnation in compatible polymer matrixes.

Conclusions

Ion−dipole interactions between the quaternary ammonium in DODAB and the carbonyl moiety in PMMA plus other weak but cooperative van der Waals interactions led to hybrid materials where DODAB was found well-dispersed in the solid polymeric matrix. This allowed combining the bactericidal DODAB property with excellent DODAB immobilization in the PMMA polymeric network. For the PS-DODAB material, however, the quoted interactions were weaker or absent and phase separation took place.

DODAB self-assembly from bilayer fragments or vesicles at oppositely charged polymeric films led to different assemblies depending on concentration of NaCl added to the vesicles.[53,57] Salt concentrations previously shown to induce intervesicle fusion favored also vesicle fusion to the air−water and to the flat polymer−water interfaces. However, in pure water, the electrostatic attraction was not enough to deposit a DODAB bilayer on polystyrene sulfate films.[53] Therefore, the mechanical approach described in this work for immobilization of the antimicrobial DODAB lipid in a polymeric network certainly represents a significant improvement regarding its applications to produce antimicrobial coatings.

Acknowledgment. Fundação de Amparo à Pesquisa do Estado de São Paulo (FAPESP) and Conselho Nacional de Desenvolvimento Científico e Tecnológico (CNPq) are gratefully acknowledged for financial support.

Supporting Information Available: The nonlinear dependence between refractive index and PS content for hybrid PS-DODAB films spin-coated onto silicon wafers and AFM phase images for hybrid films. This information is available free of charge via the Internet at http://pubs.acs.org.

References and Notes

(1) Wagner, M. L.; Tamm, L. K. *Biophys. J.* **2001**, *81*, 266–275.
(2) Shao, Z. F.; Yang, J. *Q. Rev. Biophys.* **1995**, *28*, 195–251.
(3) Salafsky, J.; Groves, J. T.; Boxer, S. G. *Biochemistry* **1996**, *35*, 14773–14781.
(4) Sicchierolli, S. M.; Carmona-Ribeiro, A. M. *J. Phys. Chem.* **1996**, *100*, 16771–16775.
(5) Steinem, C.; Janshoff, A.; Ulrich, W. P.; Sieber, M.; Galla, H. J. *Biochim. Biophys. Acta* **1996**, *1279*, 169–180.
(6) Glazier, S. A.; Vanderah, D. J.; Plant, A. L.; Bayley, H.; Valincius, G.; Kasianowicz, J. J. *Langmuir* **2000**, *16*, 10428–10435.
(7) Carmona-Ribeiro, A. M. *Chem. Soc. Rev.* **2001**, *30*, 241–247.
(8) Puu, G.; Artursson, E.; Gustafson, I.; Lundstrom, M.; Jass, J. *Biosensors & Bioelectron.* **2000**, *15*, 31–41.
(9) Carmona-Ribeiro, A. M. In *Handbook of Surfaces and Interfaces of Materials*; Nalwa, H. S., Ed.; Academic Press: San Diego, 2001; Vol. 5, Chapter 4.
(10) Tamm, L. K.; McConnell, H. M. *Biophys. J.* **1985**, *47*, 105–113.
(11) Horn, R. G. *Biochim. Biophys. Acta* **1984**, *778*, 224–228.
(12) Marra, J.; Israelachvili, J. *Biochemistry* **1985**, *24*, 4608–4618.
(13) Pashley, R. M.; McGuiggan, P. M.; Ninham, B. W.; Brady, J.; Evans, D. F. *J. Phys. Chem.* **1986**, *90*, 1637–1642.
(14) Sackmann, E. *Science* **1996**, *271*, 43–48.
(15) Moya, S.; Donath, E.; Sukhorukov, G. B.; Auch, M.; Baumler, H.; Lichtenfeld, H.; Mohwald, H. *Macromolecules* **2000**, *33*, 4538–4544.
(16) Pereira, E. M. A.; Vieira, D. B.; Carmona-Ribeiro, A. M. *J. Phys. Chem. B* **2004**, *108*, 11490–11495.
(17) Seitz, M.; Park, C. K.; Wong, J. Y.; Israelachvili, J. N. *Langmuir* **2001**, *17*, 4616–4626.
(18) Wong, J. Y.; Majewski, J.; Seitz, M.; Park, C. K.; Israelachvili, J. N.; Smith, G. S. *Biophys. J.* **1999**, *77*, 1445–1457.
(19) Martins, L. M. S.; Mamizuka, E. M.; Carmona-Ribeiro, A. M. *Langmuir* **1997**, *13*, 5583–5587.
(20) Campanhã, M. T. N.; Mamizuka, E. M.; Carmona-Ribeiro, A. M. *J. Phys. Chem.* **2001**, *105*, 8230.
(21) Carmona-Ribeiro, A. M.; Ortis, F.; Schumacher, R. I.; Armelin, M. C. S. *Langmuir* **1997**, *13*, 2215–2218.
(22) Esumi, K.; Sugimura, A.; Yamada, T.; Meguro, K. *Colloids Surf.* **1992**, *62*, 249–254.
(23) Bayerl, T. M.; Bloom, M. *Biophys. J.* **1990**, *58*, 357–362.
(24) Rapuano, R.; Carmona-Ribeiro, A. M. *J. Colloid Interface Sci.* **1997**, *193*, 104–111.
(25) Rapuano, R.; Carmona-Ribeiro, A. M. *J. Colloid Interface Sci.* **2000**, *226*, 299–307.
(26) Scott, M. J.; Jones, M. N. *Colloid Surface A* **2001**, *182*, 247–256.
(27) Jackson, S.; Reboiras, M. D.; Lyle, I. G.; Jones, M. N. *Faraday Discuss. Chem. Soc.* **1986**, *85*, 291–301.
(28) Bennett, T. C.; Creeth, J. E.; Jones, M. N. *J. Liposome Res.* **2000**, *10*, 303–320.
(29) Carmona-Ribeiro, A. M.; Midmore, B. R. *Langmuir* **1992**, *8*, 801–806.

(30) Tsuruta, L. R.; Lessa, M. M.; Carmona-Ribeiro, A. M. *J. Colloid Interface Sci.* **1995**, *175*, 470–475.

(31) Carmona-Ribeiro, A. M.; Lessa, M. D. *Colloid Surface A* **1999**, *153*, 355–361.

(32) Knoll, W.; Frank, C. W.; Heibel, C.; Naumann, R.; Offenhausser, A.; Ruhe, J.; Schmidt, E. K.; Shen, W. W.; Sinner, A. *Rev. Mol. Biotech.* **2000**, *74*, 137–158.

(33) Taguchi, K; Yano, S.; Hiratani, K; Minoura, N.; Okahata, Y. *Macromolecules* **1988**, *21*, 3336–3368.

(34) Taguchi, K; Yano, S.; Hiratani, K.; Minoura, N. *Macromolecules* **1991**, *24*, 5192–5195.

(35) Hillebrandt, H; Tanaka, M.; Sackmann, E. *J. Phys. Chem. B* **2002**, *106*, 477–486.

(36) Imberg, A; Hansson, P. *J. Phys. Chem. B* **2005**, *109*, 10830–10834.

(37) Lestage, D. J.; Min, Y.; Urban, M. W. *Biomacromolecules* **2005**, *6*, 1561–1572.

(38) Kuegler, R.; Bouloussa, O.; Rondelez, F. *Microbiology* **2005**, *151*, 1341–1348.

(39) Vieira, D. B.; Carmona-Ribeiro, A M. *J. Antimicrob. Chemo.* **2006**, *58*, 760–767.

(40) Carmona-Ribeiro, A. M.; Vieira, D. B.; Lincopan, N. *Anti-Infective Agents in Medicinal Chemistry* **2006**, *5*, 33–54.

(41) Carmona-Ribeiro, A M. *Curr. Med. Chem.* **2006**, *13*, 1359–1370.

(42) Elias, H.-G. *An Introduction to Polymer Science*, 1st ed.; VCH: New York, 1997; Chapter 1.

(43) Mennicke, U.; Salditt, T. *Langmuir* **2002**, *18*, 8172–8177.

(44) Baumgart, T.; Offenhaeusser, A. *Langmuir* **2003**, *19* (5), 1730–1737.

(45) Salditt, T.; Pfeiffer, F.; Perzl, H.; Vix, A.; Mennicke, U.; Jarre, A.; Mazuelas, A.; Metzger, T. H. *Physica B* **2003**, *336*, 181–192.

(46) Simonsen, A. C.; Bagatolli, L. A. *Langmuir* **2004**, *20*, 9720–9728.

(47) Generosi, J.; Castellano, C.; Pozzi, D.; Castellano, A. C.; Felici, R.; Natali, F.; Fragneto, G. *J. Appl. Phys.* **2004**, *96*, 6839–6844.

(48) Estes, D. J.; Mayer, M. *Colloid Surface B* **2005**, *42*, 115–123.

(49) Pompeo, G.; Girasole, M.; Cricenti, A.; Cattaruzza, F.; Flamini, A.; Prosperi, T.; Generosi, J.; Congiu Castellano, A. *Biochim. Biophys. Acta* **2005**, *1712*, 29–36.

(50) Estes, D. J.; Lopez, S. R.; Fuller, A. O.; Mayer, M. *Biophys. J.* **2006**, *91*, 233–243.

(51) Walsh, C. B; Franses, E. I. *Thin Solid Films* **2003**, *71*, 429–435.

(52) Schubert, D. W. *Polymer Bull.* **1997**, *38*, 177–182.

(53) Pereira, E. M. A.; Petri, D. F. S.; Carmona-Ribeiro, A. M. *J. Phys. Chem. B* **2002**, *106*, 8762–8767.

(54) Petri, D. F. S. *J. Braz. Chem. Soc.* **2002**, *13*, 695–699.

(55) Azzam, R. M. A.; Bashara, N. M. *Ellipsometry and Polarized Light*; North Holland: Amsterdam, 1987.

(56) Palik, E. D. *Handbook of Optical Constants of Solids*; Academic Press, Inc.: London, 1985..

(57) Pereira, E. M. A.; Petri, D. F. S.; Carmona-Ribeiro, A. M. *J. Phys. Chem. B* **2006**, *110*, 10070–10074.

(58) Petri, D. F. S.; Pereira, E. M. A.; Carmona-Ribeiro, A. M. In *Contact Angle, Wettability & Adhesion* Vol. 2, K. L. Mittal, Ed.; VSP, 2002; pp 535−548..

(59) Castro, L. B. R.; Almeida, A. T.; Petri, D. F. S. *Langmuir* **2004**, *20*, 7610–7615.

(60) Atkins, P. W. *Physical Chemistry, 5th* ed., Oxford University Press: Tokyo, 1994; Chapter 7.

(61) Vaara, M. *Microbiol. Rev* **1992**, *56*, 395–411.

(62) Campanhã, M. T. N.; Mamizuka, E. M.; Carmona-Ribeiro, A. M. *J. Lipid Res.* **1999**, *40*, 1495–1500.

(63) Cutter, C. N.; Willett, J. L.; Siragusa, G. R. *Lett. Appl. Microbiol.* **2001**, *33*, 325–328.

JP801297T